

# Synthesis, Characterization And Application Of Nano Bound Terpolymer

A. Neela, V. Rama

**Abstract:** This study deals with the encapsulation of copper oxide nanoparticles with a terpolymer resin by ultrasonic irradiation technique. The plant-mediated biological synthesis of copper oxide nanoparticles involves the addition of 1mmol solution of copper chloride to 30 mL of Acacia catechu (Karungali) plant extract at 60°C, which acts as a biological reducing agent. The resultant brown nano powder is characterized by using various analytical techniques, such as Fourier Transform Infrared spectroscopy, X-ray diffraction, Scanning Electron Microscopy and Transmission Electron Microscopy. In this method, encapsulation involves dissolution of nano copper oxide into one of the monomers trioxane followed by conventional condensation by refluxing 4-hydroxyacetophenone and melamine in the presence of 2M HCl as a catalyst in temperature range of 123-130°C. After the completion of the reaction, terpolymer incorporated with nano copper oxide is purified by dissolution in 8% NaOH, re-precipitated by dropwise addition of 1:1 2M HCl and then characterized by different spectral methods like FT-IR, TGA - DTA, Proton NMR and Carbon -13 NMR to elucidate the structure of the CuO/HAMT nanocomposite. In addition, both terpolymer and the nano bound terpolymer are investigated for the anti-oxidant activity using 2,2-diphenyl,1-picryl hydrazyl (DPPH). From the result, it is found that the incorporated terpolymer is more effective scavenger of DPPH than the polymer.

**Index terms:** Anti-oxidant activity, Cationic condensation, Encapsulation, Nano composite, Reducing agent, Terpolymer, Ultrasonic irradiation.

## 1 INTRODUCTION

Polymers are considered to be good hosting matrices for composite materials because they can easily be tailored to yield a variety of bulk physical properties. Moreover, organic polymers generally have long-term stability and good process ability. Inorganic nanoparticles possess outstanding optical, catalytic, electronic and magnetic properties, which are significantly different their bulk states. By combining the attractive functionalities of both components, nanocomposites derived from organic polymers and inorganic nanoparticles are expected to display synergistically improved properties. polymer matrix-based nanocomposites have become a prominent area of current research and development. Exfoliated clay-based nanocomposites have dominated the polymer literature but there are a large number of other significant areas of current and emerging interest. A long term review shows the preparation of nano composites like HfO<sub>2</sub>, ZrO<sub>2</sub>, ZnO, Fe<sub>2</sub>O<sub>3</sub>, TiO<sub>2</sub>, Al<sub>2</sub>O<sub>3</sub>; MMA; Fluoropolymers[1], Fe<sub>2</sub>O<sub>3</sub>; Modified PMMA[2], Fe<sub>2</sub>O<sub>3</sub>; Initiator plus styrene[3], Al<sub>2</sub>O<sub>3</sub>; Polyacrylic acid [4], Al<sub>2</sub>O<sub>3</sub>; Polyethylene[5], Al<sub>2</sub>O<sub>3</sub>; Pyrrole[6], ZrO<sub>2</sub>; Polyethylene [7], TiO<sub>2</sub>; PMMA; [8], TiO<sub>2</sub>; Polystyrene [9], SiO<sub>2</sub>; Polystyrene [10], SiO<sub>2</sub>; Acrylate based polymers; [11], ZnO; Acrylic acid; [12], Fe<sub>3</sub>O<sub>4</sub>; e-Caprolactone; [13], Fe<sub>3</sub>O<sub>4</sub>; Caprolactone; [14], Tang et al [15] have reported that inclusion of dry powder SiO<sub>2</sub> particles in starch PVOH films increased tensile strength at break and improved water barrier properties. Xiong et al [16] have reported improved mechanical properties, transmittance, and water resistance of starch films containing nano-SiO<sub>2</sub> particles. This paper shows a new frontier view on the synthesis of copper oxide from the aqueous extract Acacia catechu plant and of CuO/HAMT nano composite. The experimental data indicate the formation of product and gradual change in the morphology which is essential for optimizing the processing conditions.

## 2 EXPERIMENT

### 2.1 Materials and instrumentation

All chemicals and reagents are purchased from Merck and Aldrich. FT-IR spectrum is recorded on Shimadzu FT-IR 8300 series instrument in the range of 4000-400cm<sup>-1</sup> using potassium bromide pellets. The phase identity and crystalline size of copper oxide nanoparticles are characterized by Shimadzu X-ray diffractometer (PXRD-7000) using Cu-K α-radiation of wavelength  $\lambda = 1.5406 \text{ \AA}$ . Morphological features are studied using Hitachi-7000 Scanning Electron Microscopy and Transmission electron microscopy. <sup>1</sup>H NMR and <sup>13</sup>C NMR spectra (400MHz, 100MHz) are recorded on a DRX-500 Advance Bruker spectrometer, thermal stability from TGA-DTA and Anti-oxidant activity through DPPH assay.

### 2.2 Preparation of Extract & Synthesis of Copper oxide nanoparticles

Fresh Leaves of Acacia catechu are collected, washed in running tap water and shade dried at room temperature. Dried leaves are powdered using a mixer mechanically, sieved and subjected to Soxhlet extraction using deionized water for two hours. The aqueous solution obtained after extraction is subjected to concentration under reduced pressure at 40 ± 5°C by rotary flash evaporator. To illuminate the effects of the plant extract, different concentrations (5, 10, 15, and 20 ml) are used by keeping the source of copper chloride at a constant value. In this work, the reaction mixture is prepared by adding 15 ml of the plant extract (fuel) and copper chloride (0.1 g) as a source of copper under constant stirring until the colour changes to brown. Then it is kept in a preheated muffle furnace maintained at 400 ± 10<sup>0</sup> C. Copper oxide nanoparticles are formed after 3 hours. The resultant is stored in airtight container for further analysis.

### 2.3 Preparation of CuO/HAMT nano composite

A mixture of 4-hydroxyacetophenone and Melamine in the molar ratio 1: 1 with 2M HCl is refluxed over oil bath in temperature range of 123-130<sup>0</sup> C for 8 hours with stirring. Encapsulation involves dissolution of copper oxide nanoparticle into one of the monomers trioxane. The solid

- Neela, Rani Anna Government College for women, Affiliated to M.S. University, Tamil Nadu, India., Corresponding Author: V. Rama, Department of Chemistry, Sarah Tucker College, Tirunelveli.

product so obtained is taken from the flask and kept in a sonicator of ultrasonic frequencies (>20kHz) for half an hour. It is washed with hot water, dried and powdered. After the completion of the reaction, terpolymer incorporated with copper oxide nanoparticles is purified by dissolution in 8% NaOH and reprecipitated by drop-wise addition of 1:1 2M HCl. The synthetic details are given in Table 1.

Scheme of the preparation

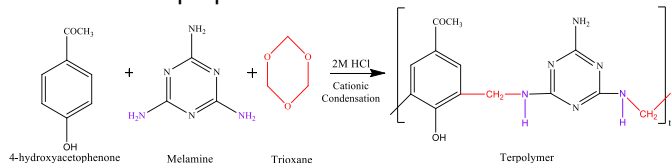


**Table 1** Synthetic details of CuO/HAMT nanocomposite

Parameters/conditions	specifications
4-hydroxyacetophenone	0.1M
Melamine	0.1M
Catalyst, 2M HCl	100mL
Trioxane	0.2M
Copper oxide nanoparticles	0.4 mg
Temperature	123-130 <sup>o</sup> C
Time	8 hours
Yield	73%

## 2.4 Anti-oxidant activity

DPPH radical scavenging activity is carried out by the method of Molyneux. To 1.0 ml of 100.0  $\mu$ M DPPH solution in methanol, equal volume of the sample in methanol of different concentration is added and incubated in dark for 30 minutes. The change in colouring is observed in terms of absorbance using a spectrometer at 514 nm. 1.0 ml of methanol instead of test sample is added to the control tube. The different concentration of Ascorbic acid is used as reference compound. Percentage of inhibition is calculated from the formula, [(Absorbance of control - Absorbance of test)/ Absorbance of control]  $\times$  100. The value of IC<sub>50</sub> was calculated using Graph pad prism 5.0.

## 3 RESULT AND DISCUSSION

### 3.1 Spectral analysis

The synthesized nano sized Copper oxide nanoparticles are characterized by X-ray diffraction study and FT-IR. Polymer and nanocomposite are characterized by spectral techniques like FT-IR, <sup>1</sup>H NMR, <sup>13</sup>C NMR to elucidate the structure of CuO/HAMT and thermal stability is done by Thermo Gravimetric Analysis.

### 3.2 X-ray diffraction study

The purity and crystallinity of the synthesized Copper oxide nanoparticles are examined using powder X-ray diffraction as shown in Fig 1. The XRD pattern shows the distinct diffraction peak with  $d=2.5270\text{\AA}$  is the characteristic peak of end centered monoclinic. The obtained data is matched with the Joint Committee on Powder Diffraction Standards file no 450937. The particle size is calculated from X-ray diffraction images of CuO powder using Scherrer's formula  $D=0.89 \lambda/\beta \cos\theta$  and found as 3.9 nm.

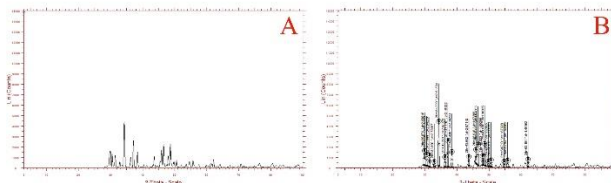


**Fig.1.** XRD Pattern of copper oxide nanoparticles

### 3.3 EDAX

The Energy Dispersive Analysis Fig 2 indicates how the concentration of elements Cu, O and C varies periodically along the size of atoms being accompanied with maxima of Cu along 72%, O along 21%, C along 7% of distributions and there is no evidence of impurity in the composition of copper oxide nanoparticles.

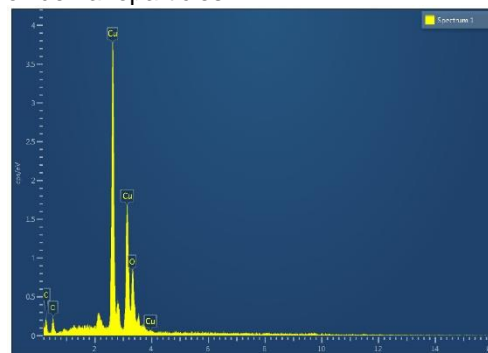


**Fig. 2.** EDAX image of copper oxide nanoparticles

### 3.4 AFM Surface Analysis

Fig 3 depicts a typical 3D AFM topographic image and its corresponding graph together of the CuO/HAMT nano composite. The surface was imaged in tapping mode. Roughness is reported in terms of several parameters over the measured area e.g. the roughness average; the root mean square; the valley value; the peak value; the range between peak and valley value. The roughness calculation parameters measured from AFM were specified in a table as tool result.

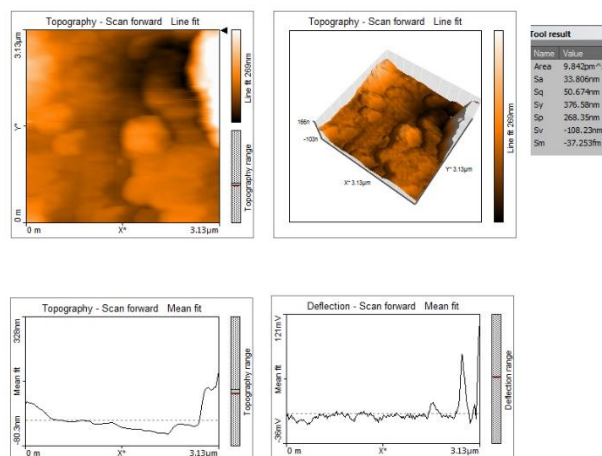


**Fig 3.** AFM Topography image of nanocomposite

### 3.5 IR Spectra

Most of the researchers[17],[18],[19],[20],[21] who prepared Copper oxide nanoparticles reported the characteristic peaks in the range of 400-650  $\text{cm}^{-1}$ , but in some other

cases [22],[23] an additional peak observed at  $1383\text{ cm}^{-1}$  was explained due to Cu-O stretching and  $583\text{ cm}^{-1}$  attributed to vibration of Cu-O. The IR spectra of Copper oxide nano particle, terpolymer and nanocomposite are depicted in Fig 4 and spectral data incorporated in Table 2. The peak observed at  $1347\text{ cm}^{-1}$  in the IR spectrum of Polymer shows the presence of methylene bridges in polymeric chains. The peak appears at  $1495\text{ cm}^{-1}$  due to -NH- bending in terpolymer. A peak at  $1613\text{ cm}^{-1}$  may be due to the stretching vibrations of  $>\text{C}=\text{N}-$ . The bands at  $853\text{-}904\text{ cm}^{-1}$ ,  $1004\text{-}1058\text{ cm}^{-1}$  and  $1125\text{-}1133\text{ cm}^{-1}$  suggest that the presence of aromatic ring is tri substituted. This presence of one isolated H atom is further confirmed by the presence of peak at  $895\text{-}955\text{ cm}^{-1}$

**Table 2** Infra-red spectral data

Sample Code	IR (Frequency $\text{cm}^{-1}$ )	Nature of fragment assigned
CuO	1383	CuO stretching
	583	Cu-O to vibration
Polymer	1347	--CH <sub>2</sub> -- bridges
	1495	-NH- bending
	3393	Phenolic -OH inter molecular bonding
Nanocomposite	1613	$>\text{C}=\text{N}-$ . stretching

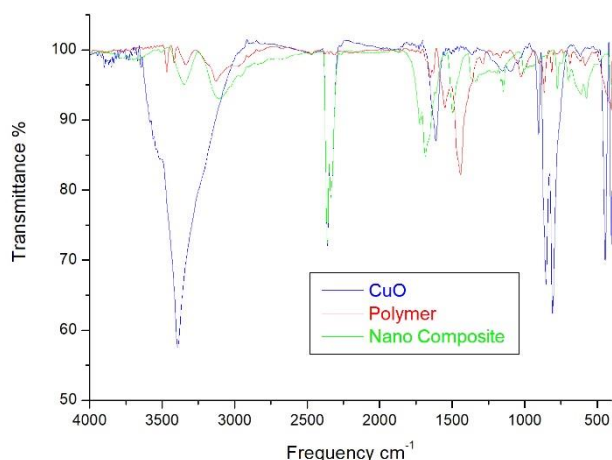


**Fig. 4.** Infrared spectra of copper nano particle, Polymer and nanocomposite

### 3.6 <sup>1</sup>H NMR and <sup>13</sup>C NMR

A depth profile of <sup>1</sup>H NMR and <sup>13</sup>C NMR spectra Fig 5 of nanocomposite show the presence of H atoms in different environments and functional groups. The data are given in the Table 3. A singlet at 2.47 ppm equivalent to 3H, represented the methyl protons attached benzoyl group. Two separate downfield multiplets between 7.343 ppm and 7.301 ppm exhibited the aromatic protons. The ortho proton is deshielded by the diamagnetic anisotropic effect of C=O group. A singlet at 6.003 ppm, equivalent to proton on the nitrogen. A peak at 120 ppm indicates aryl carbon and 129 ppm shows the presence of carbon attached with nitrogen atom. A strong peak at 167 ppm gives the idea about carbonyl carbon.

**Table 3** NMR data of nanocomposite

Sample Code	Chemical shift (ppm)	Nature of fragment assigned
Nanocomposite <sup>1</sup> H NMR	2.47	Methyl protons
	7.343 and 7.301	Aromatic protons
	6.003	Proton on nitrogen
Nanocomposite <sup>13</sup> C NMR	120, 129	Aryl carbon and Carbon attached to nitrogen Atom.
	167	Carbonyl Carbon.

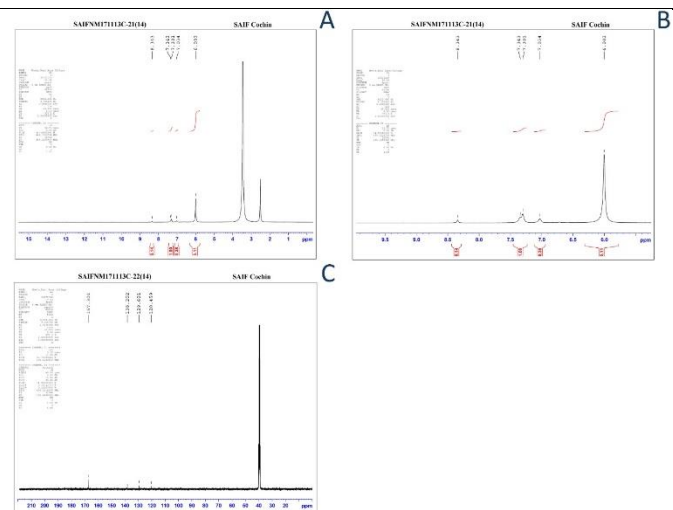


**Fig. 5.** <sup>1</sup>H NMR and <sup>13</sup>C NMR spectra of nanocomposite

### 3.7 Morphological study

A SEM with variable pressure is used to observe the morphological features of the nanocomposite. The SEM micrographs Fig 6 is recorded at magnifications of 10,000x and 15,000x. From the micrographs, it is suggested that the particles are polydispersity in nature.

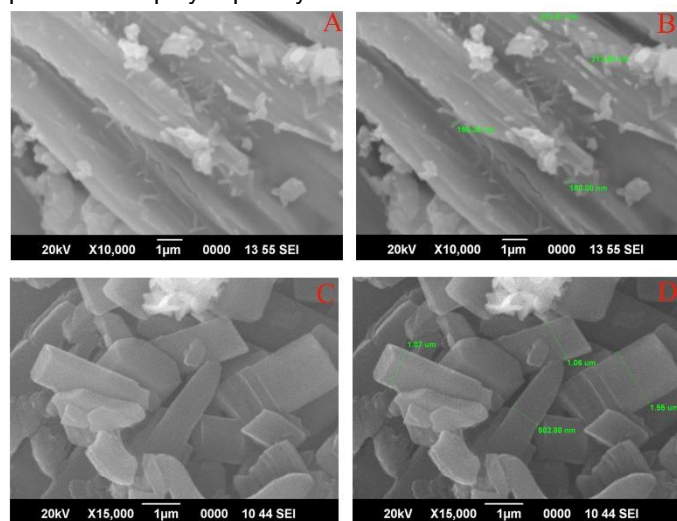


**Fig. 6.** SEM images of nanocomposite

The structure of the nanocomposite prepared with ternary self-assembly is characterized by transmission electron microscopy (TEM). TEM image Fig 7 of the nanocomposite clearly shows multiple regularly spaced layers of copper oxide nanoparticles separated by terpolymer. A selected area electron diffraction pattern suggests a typical crystal structure of (Joint Committee on

Powder Diffraction Standards [JCPDS]) which is consistent with the XRD result.

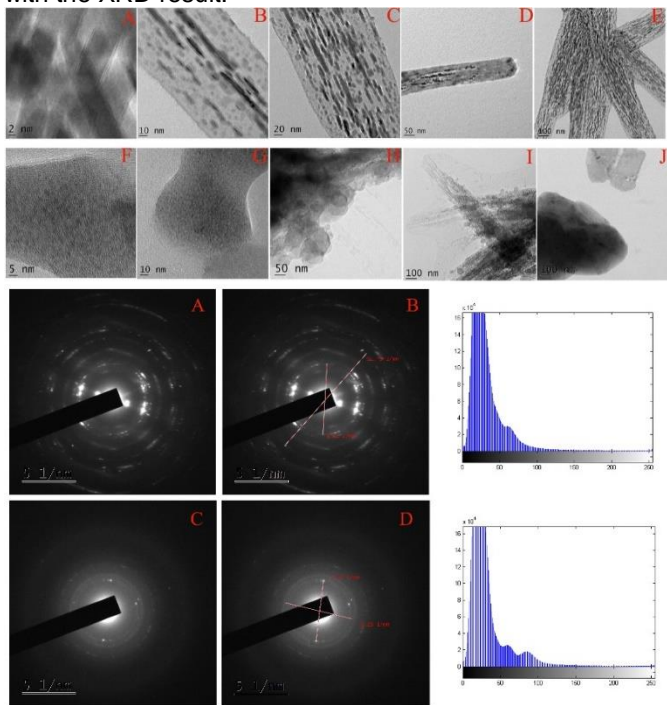


Fig.7. TEM and SAED patterns of nanocomposite

Histogram is drawn using MATLAB software on SAED pattern, indicating the number of particles distributed with respect to its size. A maximum number of particles are in the range of 10 to 12 nm. This is reasonably good concurrent with the corresponding parameter of XRD calculations obtained from Debye-Scherer equation.

**3.8 Thermal analysis**

The thermogram of CuO/HAMT nanocomposite as shown in the Fig 8 is recorded at Sophisticated Test & Instrumentation Centre, Kochi university in the inert atmosphere of Argon gas. The compound is heated from 40 to 740°C. The survey scan is run at 20°C per minute ended 100°C below and above the transition. The red weight loss curve shows the three distinct weight losses and confirms that there are three thermal events take place provided with thermal stability of the compound up to 634°C.

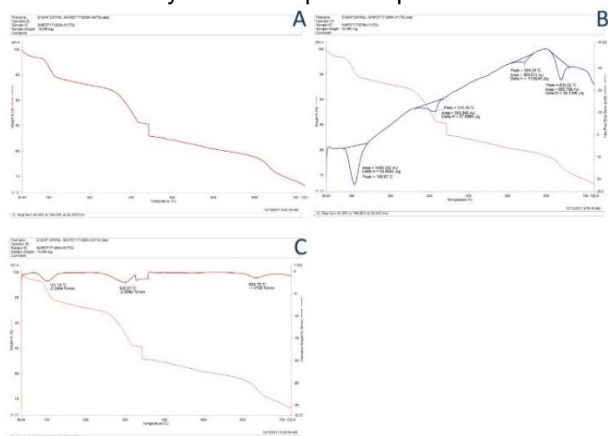


Fig. 8. Thermogram of nanocomposite

**3.9 Anti-oxidant activity**

The observed antioxidant property is due to the neutralization of the free radical character of DPPH by transfer of an electron. The variation of antioxidant activity as a function of the weight of the polymer bulk and nanocomposite has been estimated and shown in Fig 9&10. The samples quenched DPPH in a dose dependent manner; the greater the amount of material better is the DPPH scavenging ability. This is obvious because the greater the amount of the substance present, greater is the number of hydrogen atoms that can be donated for eliminating DPPH. It is observed that the antioxidant activity exhibits almost a linear variation with the amount of antioxidant present in the reaction mixture. In addition to this, comparison chart Fig 11 shows the fact that the encapsulation of copper oxide nanoparticle makes a greater number of available hydrogen atoms for eliminating DPPH, causing lesser value of IC<sub>50</sub> and making the nanocomposite with remarkable anti-oxidant property.

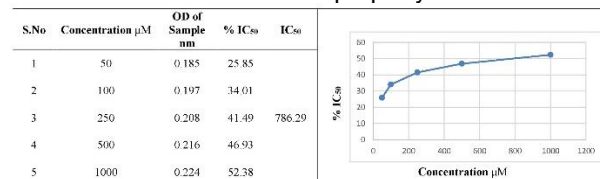


Fig. 9. Anti-oxidant activity of HAMT polymer

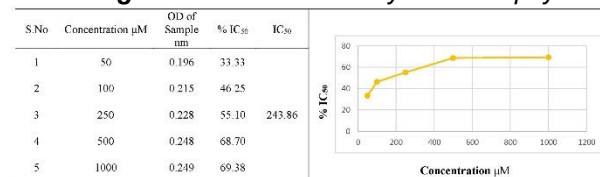


Fig. 10 Anti-oxidant activity of CuO / HAMT nanocomposite



Fig. 11. Comparison chart indicating IC<sub>50</sub> values of polymer and nanocomposite

**4 CONCLUSION**

The stimulated spirit of research on geometric dimensions below 100 nm made us to produce nano composite and to detect its fancy application as anti-oxidant agent. As a proof-of-concept, we report a new approach based on the self-assembly of metal oxide, to produce well-controlled, stable nanocomposite composed of nano copper metal oxide and HAMT. The structures of the nanocomposite prepared is characterized by FT-IR, <sup>1</sup>H NMR and <sup>13</sup>C NMR. From the scanning electron microscopy, transmission electron microscopy studies it is found that particles are polydispersity and multiple regularly spaced. We contended that strategies to coerce multiple phases of nanoscale copper oxide into deterministic nano structured materials will open new opportunities for designing multifunctional nanocomposite.

## ACKNOWLEDGMENT

The authors express their gratitude to Sarah Tucker college and Sophisticated Test & Instrumentation Centre, Kochi university for providing encouragement and available facilities.

## REFERENCES

- [1] I.Lamparth, D.V. Szabó, D. Vollath, "Nano materials: Introduction, synthesis, properties and applications", *Macromolecular Symposia*, 181, pp.107-112 2002.
- [2] D.Vollath, D.V. Szabó, J. Fuchs, "Synthesis and properties of ceramic-polymer composites", *Nano structured Materials*, 12, pp.433-438,1999.
- [3] S.M. Gravano, R. Dumas, K. Liu, T.E. Patten, "Methods for the surface functionalization of  $\gamma$ - $\text{Fe}_2\text{O}_3$  nanoparticles with initiators for atom transfer radical polymerization and the formation of core-shell inorganic-polymer structures", *Journal of Polymer Science, Polymer Chemistry*, 43, pp.3675-3688, 2005.
- [4] T.Y. Chen, P. Somasundaran, "Preparation of Novel Core-Shell Nanocomposite Particles by Controlled Polymer Bridging", *Journal of American Ceramic Society*, 1, pp. 140-144, 1998.
- [5] M.Schallehn, M. Winterer, T.E. Weirich, H. Hahn, "In situ preparation of polymer coated alumina nano powders by chemical Vapour synthesis". *Chemical Vapour. Deposition*, 9, pp.40-44, 2003.
- [6] D.Shi, P. He, S.X. Wang, W. Van Ooij, L. M. Wang, J. Zhao, Z. Yu, "Plasma deposition and characterization of acrylic acid thin film on ZnO nano particles", *Journal of Materials Research*, 17, pp.981-990, 2002.
- [7] W. He, Z. Guo, Y. Pu, L. Yan, W. Si, "Polymer coating on the surface of zirconia nano particles by inductively coupled plasma polymerization", *Applied Physics Letters*, 85, pp. 896-898, 2004.
- [8] F. Zhu, J. Zhang, Z. Yang, Y. Guo, H. Li, Y. Zhang, "Properties of monolayer black phosphorus affected by uniaxial strain", *Physica E* 27, pp. 457-461,2005.
- [9] Y. Rong, H. Z. Chen, G. Wu, M. Wang, "Preparation and characterization of titanium dioxide nano particle / polystyrene composites via radical polymerization" *Materials Chemistry and Physics*, 91, pp.370-374, 2005.
- [10] S. Gu, T. Kondo, M. Konno, "Preparation of silica-polystyrene core shell particles up to micron sizes", *Journal of Colloid and Interface Science*, 272, pp. 314-320, 2004.
- [11] J. Suffner, G. Schechner, H. Sieger, H. Hahn, "In-Situ Coating of Silica nanoparticles with Acrylate-Based Polymers," *Chemical Vapour. Deposition*, 12, pp.459-464, 2007.
- [12] D. Shi, P. He, J. Lian, L. Wang, W.van Ooij, "Plasma deposition and characterization of acrylic acid thin film on ZnO nano particles", *Journal of Materials Research*, 17, pp. 2555-2560, 2002.
- [13] A. Schmidt, "The synthesis of core-shell nanoparticles by surface initiated ring opening polymerization of  $\delta$ -caprolactone", *Macromolecular Rapid Communication*, 26, pp. 93-97, 2005.
- [14] A. Nan, R. Turcu, I. Craciunescu, O. Pana, H. Schaft, J. Liebscher, "Microwave assisted graft polymerization of  $\delta$ -caprolactone onto magnetite", *Journal of Polymer Science, Polymer Chemistry*, 47, pp. 5379-5386, 2009.
- [15] S. Z. P. Tang, H. Xiong, H. Tang, "Effect of nano- $\text{SiO}_2$  on the performance of starch/polyvinyl alcohol blend films", *Carbohydrate Polymers*, pp. 521-526,2008.
- [16] H. T.S. Xiong, H. Tang, P. Zou, "The structure and properties of a starch-based biodegradable film", *Carbohydrate Polymers*, pp. 263-268,2008.
- [17] J. Markova-Deneva, Infrared spectroscopy investigation of metallic nano particles based on copper, cobalt and nickel synthesized through borohydride reduction method", *Journal of the university of Chemical Technology and Metallurgy*, pp. 45,351, 2010.
- [18] R. Behra and G.S. Roy, "A study on sintered  $\text{TiO}_2$  and  $\text{TiO}_2/\text{SiC}$  composites synthesized through chemical reaction-based solution method", *Journal of composite materials*, 4, 26, 2012.
- [19] N.V. Suramwar S.R. Thakre and N.T. Khaty, "Synthesis and catalytic properties of nano CuO prepared by soft chemical method". *International Journal of nano Dimen*, 3,75, 2012.
- [20] A. Azam, A. S, Ahmed, M. Oves, M.S. Khan and A. Memic, "Size-dependent antimicrobial properties of CuO nanoparticles against Gram-positive and -negative bacterial strains", *International journal of nanomedicines*, 7, 3527, 2012.
- [21] A.D. Karthik and K. Geetha, "Synthesis of copper precursor, copper and its oxide nanoparticles by green chemical reduction method and its antimicrobial activity *Journal of Applied Pharmaceutical science*, 3, pp. 16, 2013.
- [22] Yu Li, "Synthesis of Copper (II) Oxide Particle and Detection of photoelectrochemically Generated Hydrogen NNIN REU Research Accomplishments", *Biological Applications*,46, 2008.
- [23] M.A. Momin, R. Pervin, M.J. Uddin, G.M.A. Khan and M. Islam, "One step synthesis and optical evaluation of copper oxide nanoparticles", *Journal of Bangladesh Electron*, 10, pp. 57, 2010.